IJCRT.ORG ISSN : 2320-2882

INTERNATIONAL JOURNAL OF CREATIVE RESEARCH THOUGHTS (IJCRT)
An International Open Access, Peer-reviewed, Refereed Journal

Analytical Investigation of Bond Strength of Concrete Filled Steel Tubes using Ansys

[1]Faiz Ahmed Shaikhbudan, [2]Chethan Kumar S, [3]Dr.N. S Kumar
[1]Student, [2]Assistant Professor, [3]Professor and Hod
[1]Dept. of Civil Engineering, [2]Dept. of Civil Engineering, [3]Dept. of Civil Engineering
[1]Dayananda Sagar College of Engineering, Bangalore, India, [2]Dayananda Sagar College of Engineering, Bangalore, India
[3]Ghousia College of Engineering, Ramanagaram, India

Abstract: A concrete-filled steel tubular (CFST) column is made by emptying concrete into a steel tube. Because of their incredible static and quake safe properties, like high strength, high pliability, enormous energy ingestion limit, twisting solidness, fire execution, and great development capacity, concrete-filled steel cylindrical (CFST) segments are presently being progressively utilized in the development of structures. The non-linear analytical research was carried out using ANSYS WORKBENCH 16, a finite element programme, to investigate the Bond strength of column filled steel tubes utilising self-compacting concrete mixes with M30, M50, M70, and normal mix with M30. The bond strength of steel and concrete has been discovered to be dependent on column diameter, length, steel tube thickness, L/D ratio, and D/t ratio.

***Index Terms* - Bond Strength, CFST column, compressive strength, ANSYS.**

I. INTRODUCTION

The steel tube filled with concrete is a composite that is presently utilized in building construction. In recent decades we have become popular with the usage of pavement steel tubular beams. The structural features of this system are good seismic-resistant such as structural applications, high ductility and high energy absorption. They consist of a circular or rectangular piece of steel hollow filled with simple or concrete columns that benefits both steel and horizontal. They are often employed as beams and beam columns in large and multi-story buildings, as beam in weak economic structures that need clear and effective complex structures.

In terms of functional efficiency and building sequencing, there are many unique benefits associated with these structural systems. Despite the existence of the concrete core, the intrinsic hump issue linked to thin wall steel tubes is avoided or postponed. In addition, owing to the impact of the containment of the stain shell, the efficiency of the infill walls is enhanced. In terms its structural performance, also the arrangement of components in the cross - sections system control extremely efficient.

1.1 BACKGROUND

The employment of enveloped or unfilled composite columns significantly reduces the size of the column compared to the columns required for the carriage of the same weight. Significant savings may thus be achieved. In case of premium level of floor space, such office complexes and parking lots, it is also beneficial to reduce the column dimension. In addition, composite columns tightly spread out of high-rise structures with spandrel beams may be utilized for the resistance to side loads via the table idea.

CFST columns prefer multiple earthquake-resistant constructions, high-rise building columns, high traffic loading bridge and railway decks columns. Baton filled tubes in stainless steel need additional fireproof insulation if the structure's fire safety is essential. Because steel tube may be utilized for coating and propping mechanism for casting the concrete in construction, the CFST structures are superior construct abilities. In addition, compared to concrete-encase steel composite sections, the CFSTs offer a strong compressive and torsi nary resistance across all axes.

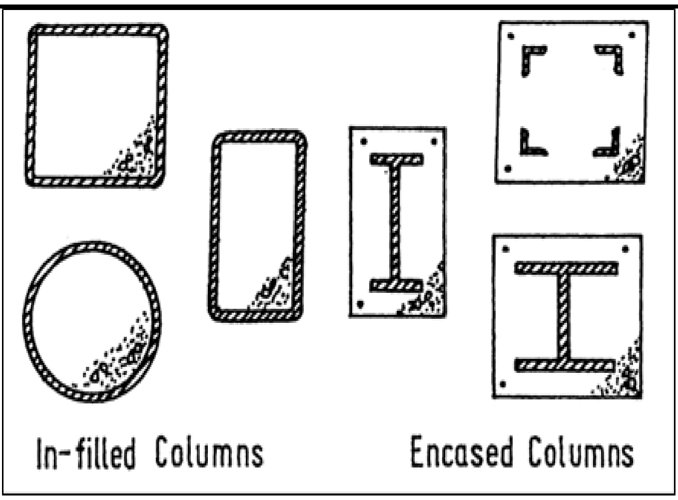

Figure 1.1: Various types of composite column

1.2 AIM

To study the structural behavior and bond strength of circular SCCFST columns with FEM Software.

II. PROPOSED OBJECTIVES

1. To use of CFST column self-compacting concrete.
2. The bond strength of circular SCCFST columns for various L/d ratios and D/T ratios are identified for analytical research.
3. To evaluation of C/S impacts on the binding strength of steel tube using ANSYS.
4. To evaluate impact on bond strength of the concrete compressive strength.

2.1 LITERATURE REVIEW

Hasan Hastemoglu, 2017 [1], studied the performance of Double Skinned Composite Columns with Concrete Filled Tubular Columns in 2007. Tubular Composite Columns with Concrete Filling Five doubly cleansed concrete filled steel circular pieces of concentrically placed roundabout regions loaded up with self-compacting concrete make up the exploratory research. The samples were put through their paces by introducing hub loads. Slimness percentage was the main test characteristic that varied between sections. The test results of DSCFT sections are compared to those of five cement-filled cylinder segments of the same steel region (Ast) and external diameter as DSCFT segments, both loaded with M50 self-compacting cement. With the help of burden diversion bends, many attributes such as firmness, malleability, and disappointment mode can be discussed. The comparison of a concrete filled cylinder to twofold cleansed concrete filled cylinder parts demonstrates that DSCFT segments are similar to CFT segments in execution and that DSCFT is more cost effective than CFT. Hypothetical research was also carried out and compared to the test outcomes. Different codes, such as EC4, LRFD, and ACI, were also examined. An ANSYS demonstration was also completed for two cases in order to change the test results obtained from tests. The results of the test study were compared to those of the ANSYS simulation. The results reveal that there isn't much of a difference in disfigurements between the ANSYS and exploratory results.

Demartinoa 2019 [2], A fiber-based FEM model is presented and subsequently verified using experimental data on the hysteresis loops of these columns in this work. The verified numerical model is then used to run a full parametric analysis to see how the major factors influencing the mechanical properties of the RAC and steel tube affect the hysteretic features of circular RACFST columns. In addition, the gathered database is utilised to undertake a grey correlation analysis with the goal of establishing measurable proof of the parametric sensitivity of circular RACFST column seismic performance. The findings of the assessment demonstrate that using the extra water method absorption of RCAs in the production of RAC decreases the lateral load capacity of the columns, but not using this technique has the opposite effect. It is also shown that the RCA % has a little impact on the seismic performance of CFSTs made with RCAs, however this influence should be taken into account during the seismic assessment.

S. Jayalekshm, J. S. Sankar Jegadesh 2016 [3], shows the numerical simulation of rectangular CFT specimens, ANSYS was used to construct a nonlinear FEM based model. The numerical model's conclusions are validated by comparing them to the available experimental data in the literature. In terms of axial capacity, there is good agreement between the experimental data and the model's output. Following parametric experiments, the constructed FE model can be used to shed more light on the extra elements impacting CFST behaviour.

The axial strength of CFST columns is estimated using codal specifications and equations. This paper presents a comparison of experimental data with numerical analysis and theoretical outcomes. Based on the findings, AISC codes have underestimated the compression capacity of CFST columns, indicating that these codes are conservative and can be employed in design because of their inherent conservatism. The influence of the D/t ratio of the columns can be attributed to the variations of the estimates from the results. There is a reduction in confinement effect when the D/t ratio is high. As a result, this article gives a thorough overview of the various international coding techniques as well as a comparative assessment of the capacity of CFST columns.

Lin-Hai Han 2007 [4], shows the conduct of cement filled meager walled steel tube individuals exposed to coupled loads like compression and torsion, bending and torsion, and compression, bending, and torsion. The limited component investigation in this work is finished with the ABAQUS program (FEA). An examination of the results determined utilizing this displaying with the test outcomes shows that they are for the most part in understanding. The impact of basic factors that influence a definitive strength of composite segments under joined stacking, like compression and torsion, bending and torsion, and compression, bending, and torsion, is then examined utilizing FEA displaying. The parametric examinations offer information for equation advancement to figure a definitive strength of composite columns presented to combined loading.

M.Pragna, Partheepan Ganesan 2016 [5], shows the load carrying capacity of concrete filled steel tubes (CFT) exposed to compression loading are presented in this work. The analysis of CFT behaviour and the different parameters that influence it is done with commercially available ANSYS, FEM software. The load carrying capability of CFT diminishes as the D/t ratio rises. It was also discovered that adding high-grade concrete as infill can boost load carrying capacity. In comparison to CFT, hollow steel has a load reduction of more than 50% at higher D/t ratios. When compared to CFT, a lower D/t ratio results in a more than 50% reduction in load capacity for hollow steel.

M.R. Bambach 2011 [6], presented the current experimental, numerical, and analytical Abaqus examinations of hollow and concrete-filled steel and stainless-steel tube members subjected to transverse impacts have yielded a number of particular results as follows, Concrete filling of metal tubes increases the bending hinge moment capacity but has minimal influence on the energy absorption capability. Enhanced stainless steel has a substantial energy absorption capability advantage over standard stainless steel, absorbing 1.8 times more energy. Simply by using the strength parameters computed during a regular static design, the maximum transverse energy capacity can be determined with accuracy and reliability. Members with no end rotational constraint absorb 18% less energy, members with no axial restraint absorb 33% less energy, and members with neither rotational nor axial restraint absorb 69 percent less energy than fully restrained members.

Pragathi. D, Sattainathan Sharma A, Aishwarya M.B 2020 [7], this paper shows analytical study on the structural behaviour between Concrete-filled double skin steel tubular (CFDST) and concrete filled steel structures (CFST) short columns with the same dimensions, the CFDST Inner Corrugated column (C) carries a higher weight than the CFST with I section (B) column. Inner Corrugation on CFDST columns has the effect of increasing the load carrying capability of the columns. Because the study's major goal is to show that CFDST columns are superior to CFST columns, it has been demonstrated that CFDST with Inner Corrugated columns can outperform CFST columns. The CFST and CFDST columns were used in this investigation, with the CFDST columns with Inner Corrugation proving to be the most cost-effective and efficient. Finally, the CFDST Inner Corrugated column is found to have a higher compression resistance than the CFST columns. These CFDST columns have been employed in high-rise bridge piers, offshore platform legs, and the construction of structures in seismically active areas.

V. G. Pawar, S. N. Patil, P. B. Salgar 2019 [9], shows the load bearing ability of light weight concrete and standard concrete with circular and rectangular column sections is investigated in this study. Various failure modes such as beam failure, column failure, and panel zone failure are discussed in this article. The infill material has an impact on the failure of beam column assemblies. Lightweight concrete is less load-bearing than regular concrete. The form of the column has an impact on failure. Infill material, specimen form, and joint type all impact strength and ductility. Steel tube strength is substantially enhanced by the form of the tube. The ANSYS programme may be used to investigate the stress distribution and failure mechanisms of concrete-filled steel tube constructions.

Xu Chang , You-Yi Wei 2011 [10],The ABAQUS/Standard solver is used to investigate the mechanical performance of SRCFST columns under cyclic loads. By comparing the computed findings to the experimental observations, the numerical method's practicality and correctness were confirmed. Based on this research, the following findings have been drawn. The addition of section steel can carry lateral loads and lessen the concrete section's tensile zone. As a result, even with the identical geometrical and material characteristics, the SRCFST columns have higher stiffness and peak lateral load than the standard CFST columns. A SRCFST column's deformation ability can also be improved by using section steel. The section steel flanges might also have a restricting impact on the concrete inner. The flanges of the section steel have the highest longitudinal stress in the concrete section of the SRCFST column.

A parametric research was also conducted, which included the effects of axial load levels, section steel ratio, section steel yield strength, concrete strength, and steel tube thickness on peak lateral load.

Zhong Tao, Brian Uy, 2009 [11], The nonlinear analysis and design of concrete-filled strengthened thin-walled steel tubular columns under axial compression are the subjects of this article. These Stub columns were subjected to further stub column testing. It shows that adding fibres to concrete or lowering its strength may efficiently enhance ductility capacity. Both techniques can be used in conjunction for constructions in high-seismic areas. In addition, the finite element analysis in this study is performed using the ABAQUS programme. A comparison of the model's results with test results reveals good agreement. The number of stiffeners improves the load-carrying capacity of steel tubes and confinement on the concrete core. It is possible to overlook the influence of residual stress on final strength. As the number of stiffeners increases, the strength loss from early flaws becomes less noticeable. Overall, the decrease effect is negligible because the concrete core contributes the majority of the final strength of a thin-walled composite specimen. Finally, the width-to-thickness ratio limit for sub-panels was examined, as well as the stiffness need for stiffeners, and suggestions were made. The load-carrying capabilities of the tested composite columns were predicted using existing design codes with minimal changes, such as AISC, BS5400, DBJ13-51-2003, and Eurocode 4. The best prediction results appear to be DBJ13-51-2003 and Eurocode 4.

III. METHODOLOGY

This chapter deals with the methodology and materials used to study the behavior of CFST columns subjected to axial loading.

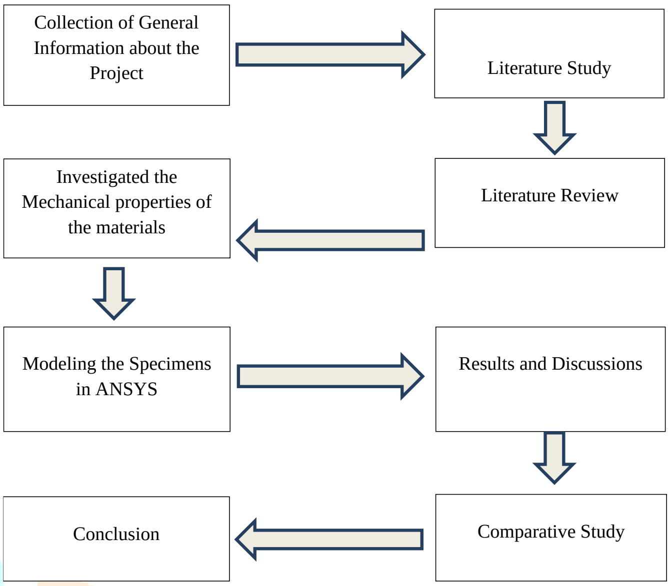

Fig.3.1. Flowchart

3.1 TAGUCHI'S METHOD

The Taguchi technique entails using a robust design of trials to reduce variance in a process. The method's overall goal is to provide a high-quality product at a cheap cost to the producer. Dr. Genichi Taguchi of Japan invented the Taguchi technique, which is being used today. Taguchi devised a technique for designing experiments to see how different factors impact the mean and variance of a process performance metric, which indicates how effectively the process is working. Taguchi's experimental design includes organising the parameters impacting the process and the levels at which they should be varied using orthogonal arrays.

3.2 FINITE ELEMENT ANALYSIS

The FEM tool ansys.16 for the purpose of simulating the CFST, CCFST, TCFST, RCFST for discretization is utilised for the analysis of the finite element The triangles are used for meshing Basic Equation Numerical [F]=[K][U] The Finite Element Analysis (FEM) is the most common means for predicting systems and structures' physical behaviour. Since analytical answers for most everyday issues in the engineering discipline are generally not accessible, numerical techniques like FEM are developed in order to discover solutions to each problem's governing equations. In recent thirty years, a great deal of research has been carried out in numerical modelling, enabling engineers to carry out simulations near to reality today.

The aim of the trial is to provide an overview of the capacity of ANSYS to produce findings as accurate as feasible for finite element analysis. ANSYS displays several features and shows what is implemented in ANSYS wherever feasible. 16, Workbench.

3.3 MODEL DETAILS

The details of these models, which have already been developed experimentally, were extracted from a journal [8], the reference for which is given below. There have been 27 models containing self-compacting concrete grades 30, 50, and 70, and three models with regular mix grade 30.

Table 3.3.1 Details of Columns

Mix	M30	SCCM30	SCCM50	SCCM70
Concrete properties				
Weight per unit volume kg/m^3	24	25	25	25
Modulus of Elasticity N/mm^2	27386.12	27386.12	35355.33	41833
Poisson's Ratio	0.2	0.2	0.2	0.2
Mix proportions				
Cement (Kg/m^3)	400	300	385	490
Fly ash (Kg/m^3)	-	123	180	160
Water(L/m^3)	209	180	197	220
CA (10 mm down) (Kg/m^3)	984	781	810	700
FA (Kg/m^3)	774	865	820	790
SP (L)	-	3.2	3.6	3.8
VMA (L)	-	0.65	0.58	0.32

Table 3.3.2 Physical & mechanical properties of galvanized steel confirming to ASTM A653 & A879

Density (kg/m3)	7800
Poisson's Ratio	0.27-0.30
Elastic Modulus (GPa)	210
Tensile Strength (Mpa)	310
Yield Strength (Mpa)	445
Elongation (%)	20

Table 3.3.3 Correction in water content

Sr. No.	Material	Property	Value
1	Structural steel	Yield stress (MPa)	265
		Ultimate strength (MPa)	410
		Young's modulus Es(MPa)	205×10^3
		Poisson's ratio µ	0.3
		Ultimate tensile strain et	0.25
2	Reinforcing bar	Yield stress (MPa)	250
		Ultimate strength (MPa)	350
		Young's modulus E_s(MPa)	200×10^3
		Poisson's ratio µ	0.3
		Ultimate tensile strain et	0.25

3.4 MODELLING IN ANSYS

NML 30

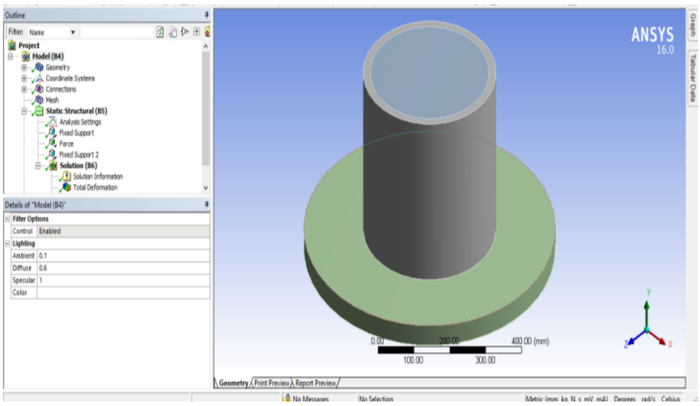

Details of "Model (B4)"

Filter Options	
Control	Enabled
Lighting	
Ambient	0.1
Diffuse	0.6
Specular	1
Color	

Fig.3.4.1. 33mm L/D 12

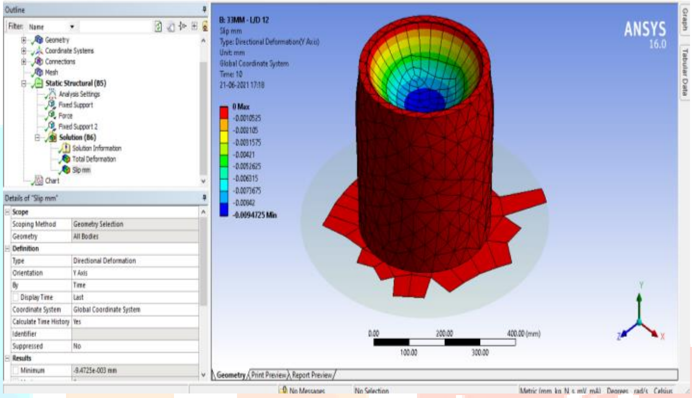

B: 33MM - L/D 12
Slip mm
Type: Directional Deformation(Y Axis)
Unit: mm
Global Coordinate System
Time: 10
21-06-2021 17:18

0 Max
-0.0010525
-0.002105
-0.0031575
-0.00421
-0.0052625
-0.006315
-0.0073675
-0.00842
-0.0094725 Min

Details of "Slip mm"

Scope	
Scoping Method	Geometry Selection
Geometry	All Bodies
Definition	
Type	Directional Deformation
Orientation	Y Axis
By	Time
☐ Display Time	Last
Coordinate System	Global Coordinate System
Calculate Time History	Yes
Identifier	
Suppressed	No
Results	
☐ Minimum	-9.4725e-003 mm

Fig.3.4.2. Slip mm: 33mm L/D 12

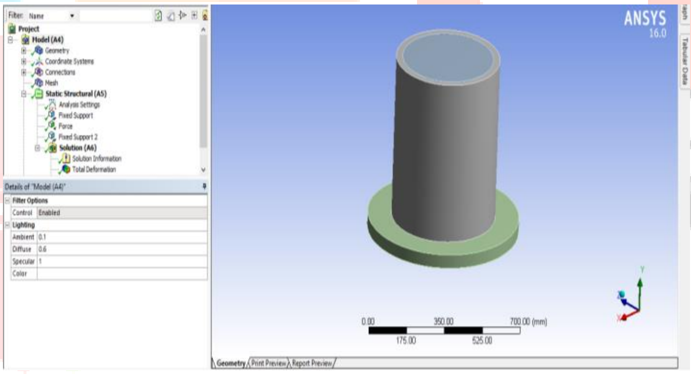

Details of "Model (A4)"

Filter Options	
Control	Enabled
Lighting	
Ambient	0.1
Diffuse	0.6
Specular	1
Color	

Fig.3.4.3. 42mm L/D 14

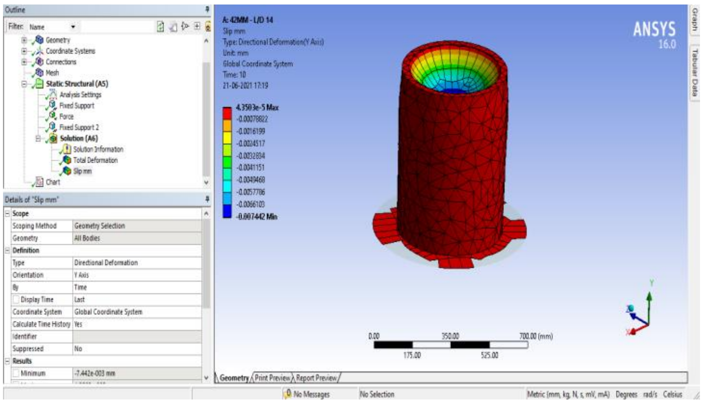

A: 42MM - L/D 14
Slip mm
Type: Directional Deformation(Y Axis)
Unit: mm
Global Coordinate System
Time: 10
21-06-2021 17:19

4.3503e-5 Max
-0.00078822
-0.0016199
-0.0024517
-0.0032834
-0.0041151
-0.0049468
-0.0057786
-0.0066103
-0.007442 Min

Details of "Slip mm"

Scope	
Scoping Method	Geometry Selection
Geometry	All Bodies
Definition	
Type	Directional Deformation
Orientation	Y Axis
By	Time
☐ Display Time	Last
Coordinate System	Global Coordinate System
Calculate Time History	Yes
Identifier	
Suppressed	No
Results	
☐ Minimum	-7.442e-003 mm

Fig.3.4.4. Slip mm: 42mm L/D 14

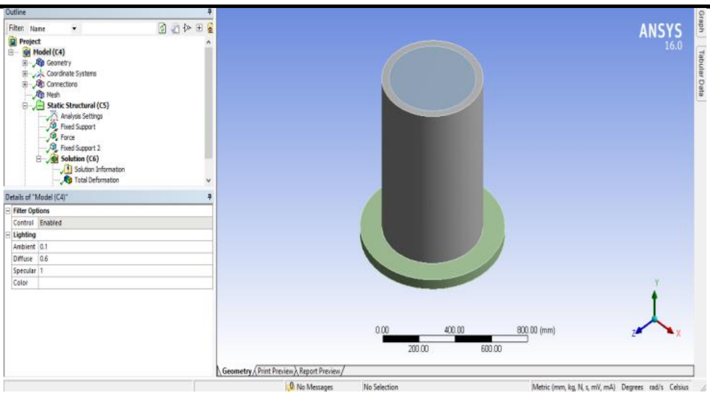

Details of "Model (C4)"

Filter Options
Control: Enabled
Lighting
Ambient: 0.1
Diffuse: 0.6
Specular: 1
Color:

Fig.3.4.5. 48mm L/D 16

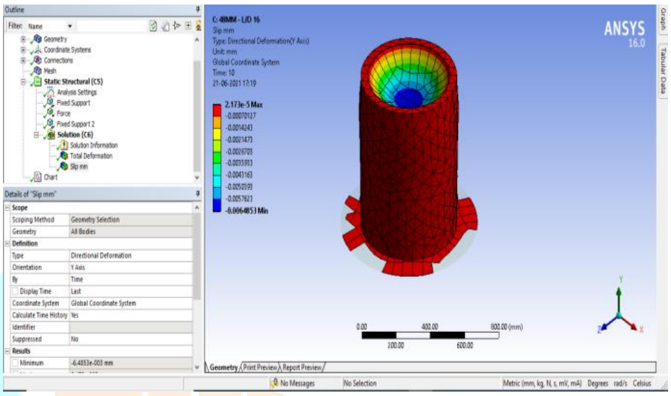

C: 48MM - L/D 16
Slip mm
Type: Directional Deformation(Y Axis)
Unit: mm
Global Coordinate System
Time: 10
21-06-2021 17:19

Details of "Slip mm"

Scope
Scoping Method: Geometry Selection
Geometry: All Bodies
Definition
Type: Directional Deformation
Orientation: Y Axis
By: Time
Display Time: Last
Coordinate System: Global Coordinate System
Calculate Time History: Yes
Identifier:
Suppressed: No
Results
Minimum: -6.4853e-003 mm

Fig.3.4.6. Slip mm: 48mm L/D 16

IV. RESULT AND DISCUSSION

Table.4.1. Results from Experimental study

Test group	Specimen label	D(mm)	t(mm)	L/D	C(Mpa)	Pu(N)	Tu(Mpa)
1	D33-L12-SCC30	33	2	12	35.4	92	3.162
	D33-L14-SCC30	33	4	14	35.4	108	3.271
	D33-L16-SCC30	33	3	16	35.4	122	3.283
2	D42-L12-SCC30	42	2	12	35.4	156	3.156
	D42-L14-SCC30	42	3	14	35.4	192	3.236
	D42-L16-SCC30	42	4	16	35.4	198	3.267
3	D48-L12-SCC30	48	4	12	35.4	192	3.133
	D48-L14-SCC30	48	3	14	35.4	248	3.216
	D48-L16-SCC30	48	2	16	35.4	300	3.221
4	D33-L12-SCC50	33	2	12	53.2	90	3.099
	D33-L14-SCC50	33	4	14	53.2	102	3.083
	D33-L16-SCC50	33	3	16	53.2	118	3.192
5	D42-L12-SCC50	42	2	12	53.2	139	2.862
	D42-L14-SCC50	42	3	14	53.2	174	2.911
	D42-L16-SCC50	42	4	16	53.2	190	3.153
6	D48-L12-SCC50	48	4	12	53.2	166	2.713
	D48-L14-SCC50	48	3	14	53.2	220	2.841
	D48-L16-SCC50	48	2	16	53.2	284	3.047
7	D33-L12-SCC70	33	2	12	71.8	86	2.941
	D33-L14-SCC70	33	4	14	71.8	98	2.994
	D33-L16-SCC70	33	3	16	71.8	100	3.11
8	D42-L12-SCC70	42	2	12	71.8	143	2.853
	D42-L14-SCC70	42	3	14	71.8	168	2.876

	D42-L16-SCC70	42	4	16	71.8	176	2.934
9	D48-L12-SCC70	48	4	12	71.8	164	2.681
	D48-L14-SCC70	48	3	14	71.8	208	2.719
	D48-L16-SCC70	48	2	16	71.8	272	2.915
10	D33-L12-SCC30	33	2	12	36.7	70	1.847
	D42-L16-SCC30	42	4	16	36.7	162	2.187
	D48-L14-SCC30	48	3	14	36.7	132	1.517

Table.4.2. Results from Analytical study

Test group	Specimen label	D(mm)	t(mm)	L/D	C(Mpa)	Pu(N)	Tu (Mpa)
1	D33-L12-SCC30	33	2	12	35.4	105.8	4.638
	D33-L14-SCC30	33	3	14	35.4	124.2	4.667
	D33-L14-SCC30	33	4	16	35.4	140.3	4.615
2	D42-L12-SCC30	42	2	12	35.4	179.4	4.858
	D42-L14-SCC30	42	3	14	35.4	220.8	5.126
	D42-L16-SCC30	42	4	16	35.4	227.7	4.624
3	D48-L12-SCC30	48	2	12	35.4	220.8	4.577
	D48-L14-SCC30	48	3	14	35.4	240	4.264
	D48-L16-SCC30	48	4	16	35.4	248	3.855
4	D33-L12-SCC50	33	2	12	53.2	103.5	4.539
	D33-L14-SCC50	33	3	14	53.2	117.3	4.41
	D33-L16-SCC50	33	4	16	53.2	135.7	4.464
5	D42-L12-SCC50	42	2	12	53.2	159.85	4.246
	D42-L14-SCC50	42	3	14	53.2	200.1	4.644
	D42-L16-SCC50	42	4	16	53.2	218.5	4.437
6	D48-L12-SCC50	48	2	12	53.2	190.9	3.956
	D48-L14-SCC50	48	3	14	53.2	237.6	4.221
	D48-L16-SCC50	48	4	16	53.2	249.4	3.8772
7	D33-L12-SCC70	33	2	12	71.8	98.9	4.338
	D33-L14-SCC70	33	3	14	71.8	112.7	4.237
	D33-L16-SCC70	33	4	16	71.8	115	3.781
8	D42-L12-SCC70	42	2	12	71.8	164.45	4.453
	D42-L14-SCC70	42	3	14	71.8	193.2	4.4838
	D42-L16-SCC70	42	4	16	71.8	202.4	4.109
9	D48-L12-SCC70	48	2	12	71.8	188.6	3.909
	D48-L14-SCC70	48	3	14	71.8	239.2	4.249
	D48-L16-SCC70	48	4	16	71.8	247.35	3.844
10	D33-L12-SCC30	33	2	12	36.7	80.5	3.529
	D42-L16-SCC30	42	3	16	36.7	186.3	4.323
	D48-L14-SCC30	48	4	14	36.7	151.8	2.359

Graphs -

The below graphs are drawn by comparing both experimental and analytical studies.

4.1 BOND STRENGTH VS DIFFERENT L/D RATIO

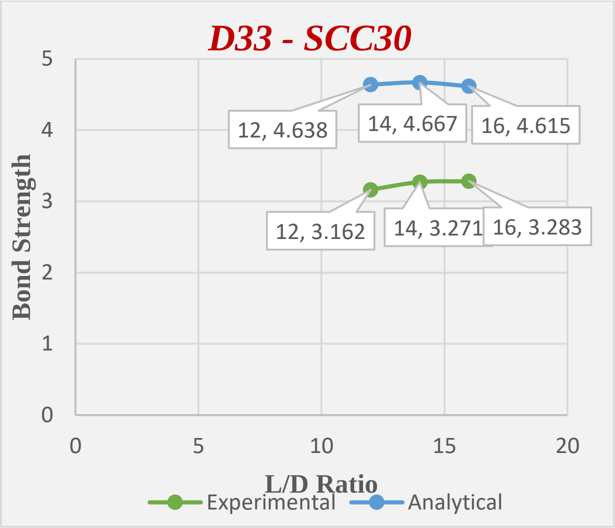

Fig.4.1.1

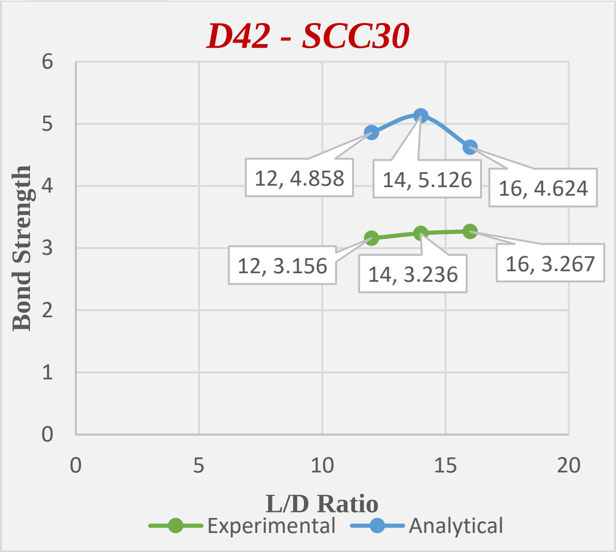

Fig.4.1.2

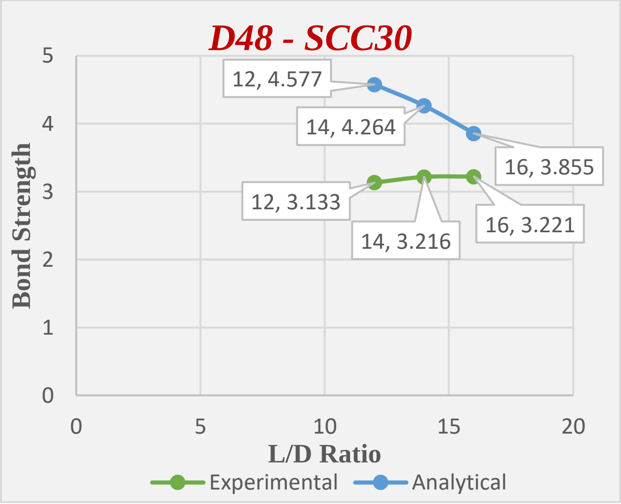

Fig.4.1.3

The above bond strength with respect to different length to diameter graphs shows increase in bond strength as follows:-

- The highest bond strength of both analytical and experimental is shown in models D42-L14-SCC30 and D33-L16-SCC30 with length to diameter of 14 and 16 is 5.126 and 3.283 respectively.
- The lowest bond strength of both analytical and experimental is shown in D48-L16-SCC30 and D48-L12-SCC30 with length to diameter of 16 and 12 is 3.855 and 3.133 respectively.

4.2 BOND STRENGTH VS DIAMETER

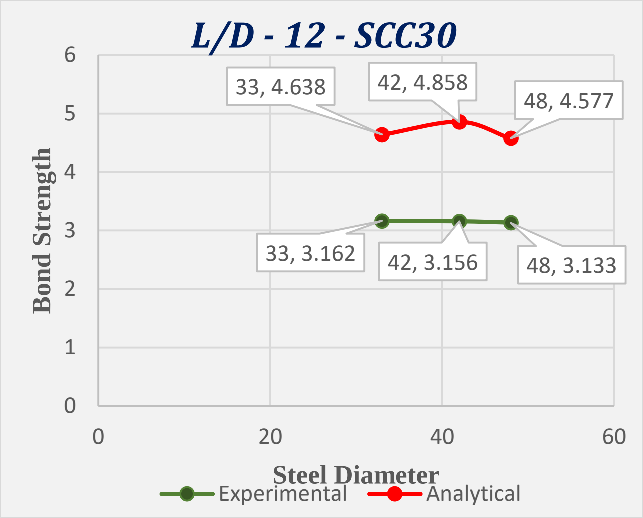

Fig.4.2.1

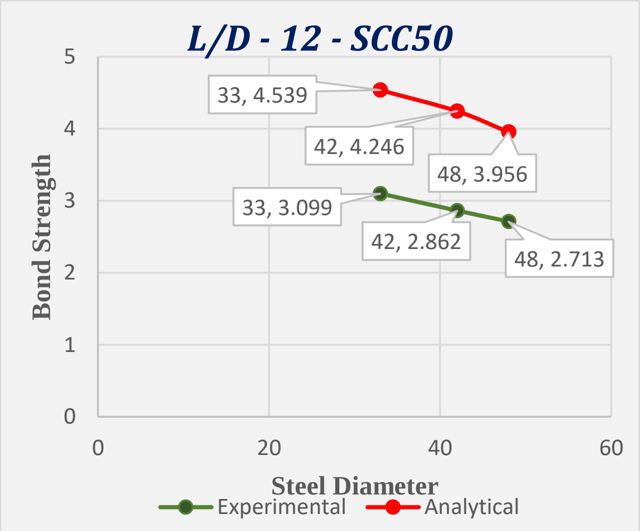

Fig.4.2.2

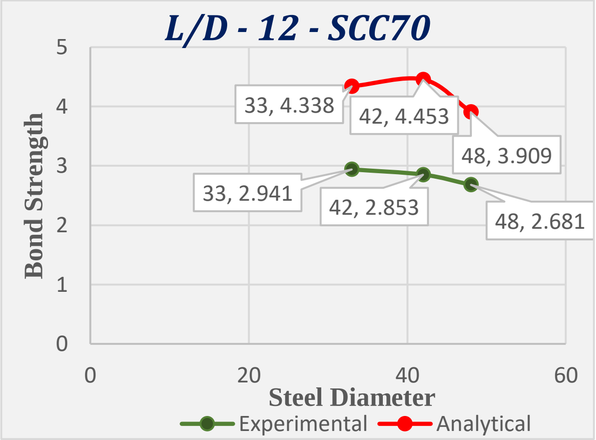

Fig.4.2.3

Comparision of bond strength in concrete filled steel tubular columns of same diameter with respect to different length to diameter as well as comparision between experimental and analytical results is shown on above graphs .The graphs shows variations in bond strength in self compacting concrete filled with steel tubular columns. The binding strength vs. diameter graph shown above demonstrates this. It can be seen that as the diameter of SCCFST columns increases, the bond strength decreases. This does not rule out the possibility that larger diameter concrete columns have lower bond strength when compared to smaller diameter specimens.

Thus, the above results can be shown below:-

- The highest bond strength of both analytical and experimental is shown in models D42-L12-SCC30 and D33-L12-SCC30 with diameter of 42 and 33 is 4.858 and 3.162 respectively.
- The lowest bond strength of both analytical and experimental is shown in D48-L12-SCC70 and D48-L12-SCC50 with diameter of 48 is 3.909 and 2.713 respectively

4.3 BOND STRENGTH VS COMPRESSIVE STRENGTH

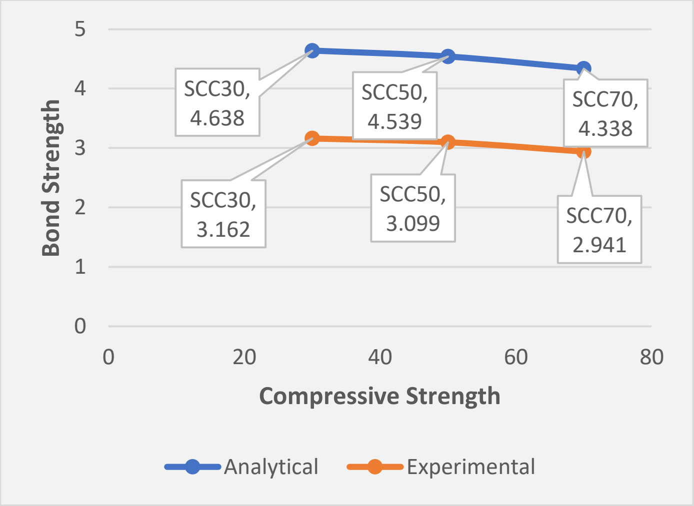

Fig.4.3.1

It can be seen that when the concrete compressive strength increases, the binding strength decreases. As a result, the bond strength of the concrete packed steel tube pillars will also depend on the concrete compressive strength.

4.4 BOND STRENGTH VS NORMAL MIX & SCC MIX

Finally, the above graph represents a comparison of the binding strength of SCCFST and traditional CFST columns. This traditional concrete filled columns were modelled of similar geometry which is shown with self-compacting concrete in block chart.

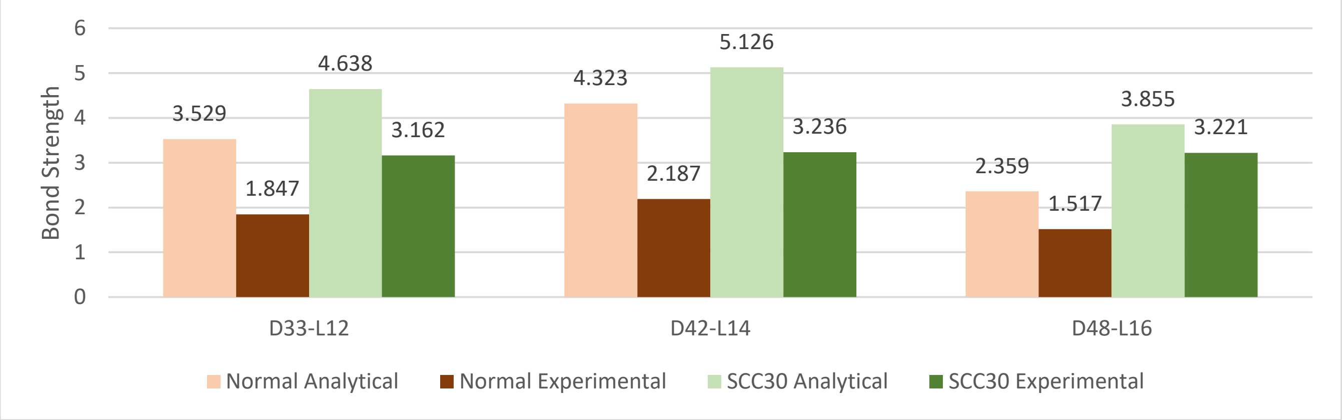

Fig.4.4.1

The above colorful block chart contains four different colors as the dark colors shows analytical and experimental of normal mix and lighter colors shows as analytical experimental of self-compacting concrete mix.

The binding strength of the self-compacting column is higher than the binding strength of the traditional concrete (NC) filled steel tube column in this comparison.

5 CONCLUSION

The data that will be gathered first from research that was carried out:

1.Through use of SCC in CFST columns does seem to have an increase in efficiency. Especially compared to the traditional CFST column, bond performance is better.

2.From the analytical work, the binding strength is reported to be influenced by the dimensions and compressive strength of the CFST columns, with either the bond strength increasing as the diameter of the steel tube and also the concrete compressive strength increases.

3.By use of SCC in CFST Columns is more profitable than using traditional CFST Columns since it has a higher bond strength and therefore does not necessitate compaction, lessening building costs and exacerbating the problem.

4.Because their tremendous bond strength, SCCFST columns perform as both a homogeneous and isotropic member, rendering CFST column successfully implementing.

REFERENCES

[1] Hastemoglu H. 2017. Behaviour of Double Skinned Composite Columns with Concrete Filled Tubular Columns. J Archit Eng Tech 6: 194.

[2] J.J. Xua, Z.P. Chenb, X.Y. Zhaoc, C. Demartinoa, T. Ozbakkaloglud, J.Y. Xuee. 2019. Seismic performance of circular recycled aggregate concrete-filled steel tubular columns: FEM modelling and sensitivity analysis. Thin-Walled Structures Volume 141, Pages 509-525.

[3] Jayalekshmi, S., Sankar Jegadesh, J. 2016. Finite Element Analysis and Codal Recommendations of Concrete Filled Steel Tubular Columns. Journal of The Institution of Engineers (India): Series A 97, 33–41.

[4] Lin-Hai Hana, Guo-Huang Yaob, Zhong Taob. 2007. Behaviours of concrete-filled steel tubular members subjected to combined loading. Thin-Walled Structures Volume 45, Issue 6, June 2007, Pages 600-619.

[5] M.Pragna, Partheepan Ganesan. (2016). Analysis of Concrete Filled Steel Tubes using Ansys. IJLERA. ISSN: 2455-7137 Volume: 01, Issue: 09, PP: 71-78.

[6] M.R. Bambach. 2011. Design of hollow and concrete filled steel and stainless-steel tubular columns for transverse impact loads. Thin-walled Structures Volume 49, Issue 10, Pages 1251-1260

[7] Pragathi D, Sattainathan Sharma. A, Aishwarya M.B. 2020. Analytical Assessment on the Structural Behaviour of CFST and CFDST Short Columns using Ansys. Volume-9, Issue-1, ISSN: 2277-3878.

[8] Shivadarshan , Chethan Kumar , Dr. N. S. Kumar. 2019. International Research Journal of Engineering and Technology (IRJET). ISSN: 2395-0056. Volume: 06 Issue: 07.

[9] V. G. Pawar, S. N. Patil, P. B. Salgar. 2019. A Study on Concrete Filled Steel Tubular Column Steel Beam Connection Using Light Weight concrete and Normal Concrete. Volume: 06 Issue: 03

[10] Xu Chang, You-Yi Wei, Yan-Chun Yun. 2011. Analysis of steel-reinforced concrete-filled steel tubular (SRCFST) columns under cyclic loading. Construction and Building Materials. Volume 28, Issue 1, March 2012, Pages 88-95.

[11] Zhong Tao, Brian Uy , Lin-Hai Han , Zhi-Bin Wang. 2009. Analysis and design of concrete-filled stiffened thin-walled steel tubular columns under axial compression. Thin-walled Structures Volume 47, Issue 12, December 2009, Pages 1544-1556.